Biophysical Chemistry 155 (2011) 29–35

Contents lists available at ScienceDirect

Biophysical Chemistry

journal homepage: http://www.elsevier.com/locate/biophyschem

The circular dichroism and differential scanning calorimetry study of the properties of DNA aptamer dimers

Slavomíra Poniková [a], Katarína Tlučková [b], Marián Antalík [b,c], Viktor Víglaský [b], Tibor Hianik [a,*]

[a] Department of Nuclear Physics and Biophysics, Faculty of Mathematics, Physics and Informatics, Comenius University, 842 48 Bratislava, Slovakia
[b] Department of Biochemistry, Faculty of Science, UPJŠ, 040 01 Košice, Slovakia
[c] Department of Biophysics, Institute of Experimental Physics SAS, 04001 Košice, Slovakia

ARTICLE INFO

Article history:
Received 7 October 2009
Received in revised form 4 February 2011
Accepted 16 February 2011
Available online 21 February 2011

Keywords:
DNA aptamer dimers
Guanine quadruplex
Thrombin
Circular dichroism
Differential scanning calorimetry
Temperature-gradient gel electrophoresis

ABSTRACT

We have applied circular dichroism (CD), temperature-gradient gel electrophoresis (TGGE) and differential scanning calorimetry (DSC) to study the properties of novel bioengineered DNA aptamer dimers sensitive to fibrinogen (F) and heparin (H) binding sites of thrombin and compared them with canonical single stranded aptamer sensitive to fibrinogen binding site of thrombin (Fibri). The homodimer (FF) and heterodimer (FH) aptamers were constructed based on hybridization of their supported parts. CD results showed that both FF and FH dimers form stable guanine quadruplexes in the presence of potassium ions like those in Fibri. The thermal stability of aptamer dimers was slightly lower compared to those of canonical aptamers, but sufficient for practical applications. Both FF and FH aptamer dimers exhibited a potassium-dependent inhibitory effect on thrombin-mediated fibrin gel formation, which was on average two-fold higher than those of canonical single stranded Fibri aptamers.

1. Introduction

DNA/RNA aptamers are single stranded oligonucleotides that at certain conditions form specific binding motifs to proteins or other ligands. Aptamers are selected in vitro by means of SELEX (systematic evolution of ligands by exponential enrichment) [1,2]. They are characterized by high affinity and specificity to their ligands, comparable with those of antibodies. Nowadays, increased interest in aptamer research is focused on improvement of these features for application in medical therapy, biotechnology and biosensor development [3,4]. A novel approach in aptamer engineering is based on dimerization [5–7] or multimerization [8], which possesses two or more binding sites for the target ligand. Among DNA aptamers, those sensitive to thrombin are most studied. Thrombin is a multifunctional serine protease that plays an important role in procoagulant and anticoagulant functions. Thrombin converts soluble fibrinogen to insoluble fibrin that forms the fibrin gel, which is responsible either for a physiological plug or for pathological thrombus [9]. This process is catalyzed by a positively charged fibrinogen-binding site within the thrombin molecule. The more positive heparin-binding site is responsible for anticoagulant functions. These binding sites are spatially separated and localized at opposite poles of the thrombin molecule. So far, two types of DNA aptamers sensitive to thrombin were developed. Initially, Bock et al. [10] developed a 15-mer DNA aptamer, which selectively binds the fibrinogen site of the thrombin. In this aptamer the intramolecular G-quadruplex plays the crucial role. According to NMR studies [11] and X-ray crystallography [12], the eight guanine residues form G tetrads that are connected at one end by TT loop and at the other end by the TGT loop (see Fig. 1). The structure of this aptamer is stabilized by K^+ ions. Later, Tasset et al. [13] developed 29-mer aptamer that selectively recognizes the heparin-binding site with considerably higher affinity to thrombin. The G-quadruplex also represents an important part of this aptamers. The substantial difference between these aptamers consists in replacement of T with A in a quadruplex loop. Earlier, circular dichroism (CD) and differential scanning calorimetry methods were shown to be sensitive tools for examining the stability of fibrinogen-specific binding site G-quadruplexes in the presence of potassium or other ions (see for example [15]) or thrombin [16]. Using CD, we showed that also the G-quadruplex forming binding motif at the heparin-binding site on thrombin is stable [14]. Recently, we proposed a simple method for aptamer engineering based on DNA hybridization of the supporting part of the DNA aptamers. This results in the formation of an aptamer dimer, so called here an aptabody, analogous to antibodies, which also possesses two binding sites [5]. In comparison to canonical aptamers with one binding site, the aptamer dimers display better detection limit and binding constant to human thrombin [5]. It has been also shown that engineered aptamers like multivalent circular constructs exhibit increased stability against cleavage by exonucleases and improved (2- to 3-fold) anticoagulant activity in comparison with canonical single stranded aptamers [8]. Increased inhibitory activity against HIV-1

* Corresponding author. Tel.: +421 2 60295683; fax: +421 2 65412305.
E-mail address: tibor.hianik@fmph.uniba.sk (T. Hianik).

0301-4622/$ – see front matter © 2011 Elsevier B.V. All rights reserved.
doi:10.1016/j.bpc.2011.02.004

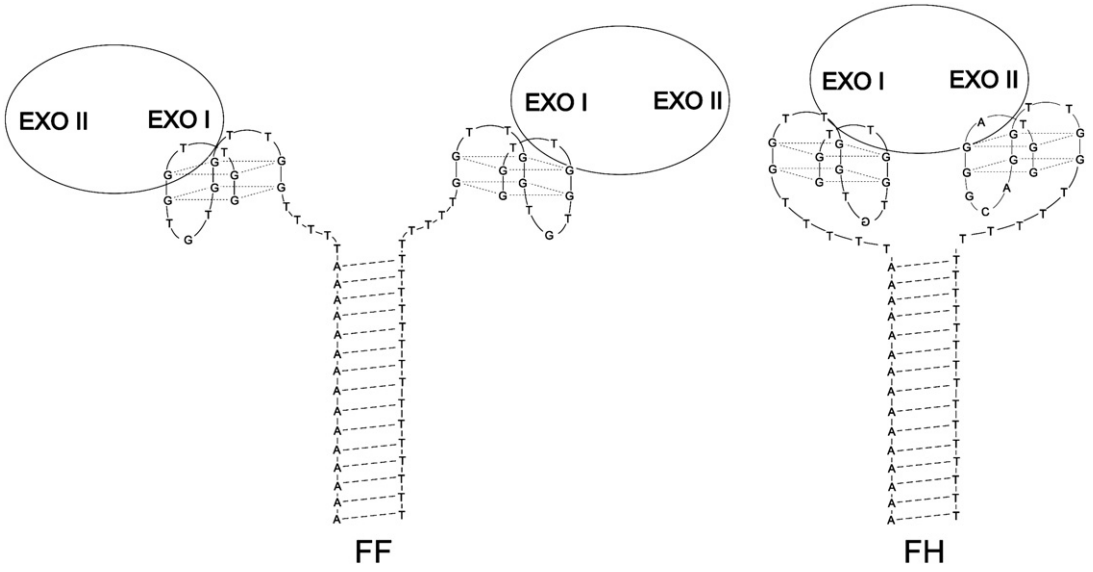

Fig. 1. Structures of FF and FH aptamer dimers bound to thrombin molecules. EXO I on thrombin molecule represents fibrinogen-recognition exosites; EXO II represents heparin-binding exosite.

reverse transcriptase has been shown also for recently reported bimodular DNA aptamers [7].

However, the properties of G-quadruplexes in aptamer dimers have not been studied previously. To the best of our knowledge, the canonical aptamer and aptamer dimer inhibition of thrombin-mediated fibrin clot formation has not yet been compared experimentally. This work is focused on the study of the properties of these novel thrombin-binding aptamer dimers. We report conformation, thermodynamic stability and the anticoagulation activity of two types of aptamer dimers and comparison of their properties with original thrombin-binding aptamer (monomer) [10]. The first type of aptamer dimer (FF aptamer dimer) is a homodimer constructed of two hybridized DNA strands, both having fibrinogen-binding site sensitive heads (Fibri). Fibri is a 15-mer nucleotide sequence that recognizes and specifically binds at fibrinogen-recognition site on thrombin [17]. On the other hand, the second aptamer dimer (FH aptamer dimer) is constructed as a heterodimer with Fibri and Hepa heads. Binding motif of Hepa is also a 15 nucleotide sequence specific to heparin-binding site on thrombin [13] (see Fig. 1). We showed that both FF and FH aptamer dimers form stable guanine quadruplexes at presence of potassium ions and exhibited potassium-dependent inhibitory effect on thrombin-mediated fibrin gel formation which is on average two-fold higher in comparison with canonical single stranded aptamers.

2. Experimental

2.1. DNA aptamers and chemicals

HPLC purified oligonucleotides were purchased from Thermo Fisher Scientific GmbH (Ulm, Germany). The concentration of oligonucleotide solutions was determined by measurement of absorbance at 260 nm using a molar extinction coefficient shown in Table 1.

Inorganic salts (p.a. grade), human plasma fibrinogen and human α-thrombin were purchased from Sigma (St. Louis, MO, USA) and used without further purification. The aptamers homodimer composed of FibriAT + FibriTT and aptamer heterodimers composed of FibriAT + HepaTT were prepared by dimerisation of their complementary supporting part. For this purpose the 1:1 mixture of both aptamers of the same concentration (5 μM for CD, 250 μM for DSC, 0.25 μM for PAGE and 2 μM for TGGE experiments) was placed in Eppendorf tube. The mixture was heated up to 95 °C and then allowed to cool at ambient temperature (25 °C). This process ensures formation of proper DNA duplex at supporting part of aptamers.

2.2. Circular dichroism polarimetry

Circular dichroism (CD) spectra were measured by JASCO J-810 spectropolarimeter (Japan) equipped with a Peltier heating/cooling device to achieve constant temperature of 25 °C in a quartz cell with optical path length of 1 cm. The oligonucleotide concentration was 5 μM in all CD experiments. Oligonucleotides were suspended in three types of solutions: 10 mM Tris, pH 7.4; 10 mM Tris + 140 mM NaCl, pH 7.4 and binding buffer (20 mM Tris + 140 mM NaCl + 5 mM KCl + 1 mM $CaCl_2$ + 1 mM $MgCl_2$), pH 7.4. Solutions were titrated with the concentrated KCl (3 M), by stepwise addition of 2–5 μl aliquots of solution until no further changes in spectrum took place. The CD spectra were measured from 320 to 220 nm.

2.3. Differential scanning calorimetry

Differential scanning calorimetry (DSC) measurements were performed on a DASM-4 microcalorimeter (Pustchino, Russia) with a cell volume 0.47 ml, under a constant pressure of 1.5 atm. The heating rate was 0.5–2 °C/min. Oligonucleotide concentrations were 250 μM and the thermodynamic properties were studied in 10 mM Tris + 140 mM NaCl + 50 mM KCl buffer solution, pH 7.4. All heating curves were corrected using an instrument baseline obtained by heating the buffer. Data were exported to OriginPro version 7.5 (Microcal Software Inc, USA) for their deconvolution into corresponding composite transitions

Table 1
The composition of aptamers and oligonucleotides analyzed and their extinction coefficient, ε.

Aptamer/oligos	The nucleotide sequence in 5′ to 3′ direction	ε, $M^{-1}cm^{-1}$
Fibri	GGT TGG TGT GGT TGG	143 300 172
FibriAT	AAA AAA AAA AAA AAA TTT TT GGT TGG TGT GGT TGG	365 300 438
FibriTT	GGT TGG TGT GGT TGG TT TTT TTT TTT TTT TTT TTT	305 700 348
HepaTT	GGT AGG GCA GGT TGG TT TTT TTT TTT TTT TTT TTT	313 600 358
ODN-A	AAA AAA AAA AAA AAA TTT TT	223 200 276
ODN-T	TT TTT TTT T TT TTT TTT TTT	162 600 186

using a Gaussian multi-peak fitting function and evaluated as described in Ref. [18].

2.3.1. Electrophoresis

Native polyacrylamide gel electrophoresis (PAGE) was run in a temperature-controlled vertical electrophoretic apparatus (Z375039-1EA; Sigma-Aldrich, San Francisco, CA). Gel concentration was 15% (19:1 monomer to bis ratio, Applichem, Darmstadt). Only 1/20 and 1/2 of DNA per well were used for standard PAGE and TGGE, respectively, as for CD experiments. Electrophoresis was run at 15 °C for 4 h at 130 V (~8 V cm^{-1}). DNA oligomers were visualized with stains, all after the electrophoresis, and the electrophoretic record was photographed with an Olympus Camedia 3000 camera. The same temperature-gradient gel electrophoresis (TGGE) equipment has been used as described previously [19]. However, for this kind of experiment about 2–3 μg of DNA were loaded into the electrophoretic well and the electrophoretic buffer contained only 50 mM KCl. Higher concentrations of potassium ion cause a high electric current. All electrophoretic measurements were performed in modified Britton–Robinson buffer: 25 mM H_3PO_4, 25 mM boric acid, and 25 mM acetic acid supplemented with 50 mM KCl. The pH was adjusted with Tris to the final value of 7.0.

2.3.2. Inhibitory activity measurement

Canonical aptamer or aptamer dimers (final concentration 0.1 μM) and thrombin (0.8 U/ml) were incubated for 1 h at 25 °C. Next, fibrinogen (final concentration 0.3 mg/ml) was added. The effect of oligonucleotides was investigated by ability of thrombin to form fibrin gels from fibrinogen in binding buffer with 50 mM potassium salt concentration. Gels were formed directly in cuvette by addition of thrombin at time zero. Absorption changes at wavelength of 450 nm were monitored for 75 min. These results were compared with data obtained for thrombin–fibrinogen system when no inhibitor was present. The absorbance measurements were made at 25 °C by Varian Cary 100 Bio UV-VIS spectrophotometer (USA).

3. Results and discussion

3.1. CD spectral studies

In the first series of experiments we studied the ability of aptamer dimers to form guanine quadruplex motifs that are required to bind and inhibit human α-thrombin. Formation of G-quadruplex can be clearly identified by CD spectroscopy [20]. CD spectra of individual components of aptamer dimers are presented in Fig. 2. Fig. 2a shows the CD spectra of the thrombin-binding aptamer Fibri. The spectra containing the negative Cotton band with minimum around 267 nm and positive band at 292 nm are consistent with those reported in the literature for similar sequences [14–16,21] in the presence of potassium ions. Such CD pattern is observed when antiparallel G-quadruplex is formed. Hepa head is able to form G-quadruplex similarly to those of Fibri [14]. In the presence of potassium, the other three aptamers exhibited positive Cotton peaks around 292 nm and displacement of negative band from 267 to 249 nm for FibriAT (Fig. 2b) and around 260 nm for FibriTT and HepaTT (Fig. 2c and d, respectively). This displacement could be caused by flanked sequences of $dA_{15}T_5$ and dT_{20}, respectively. The comparison of these CD spectra with those for Fibri aptamer suggests folding of aptamer disordered structures to antiparallel quadruplexes for each of sequences studied in presence of potassium ions.

However, creation of aptamer dimers is accompanied by formation of duplex part of the molecule. The presence of duplex can be observed at CD spectra. Fig. 3a shows three spectra of duplex part of aptamer dimers – ODN-A:ODN-T in molar ratio 1:1. Dotted line represents disordered DNA molecules with no specific CD pattern obtained in low ionic strength of solution. Addition of 50 mM KCl supports hybridization of complementary parts of molecules (dashed line). Presence of binding buffer with substantially higher ionic strength resulted in complete hybridization that is displayed by twiddle with local minimum around 266 nm and local maximum around 259 nm. The similar twiddle pattern, but with sharpest local extremes at the same wavelengths was observed for poly(dA.dT) at

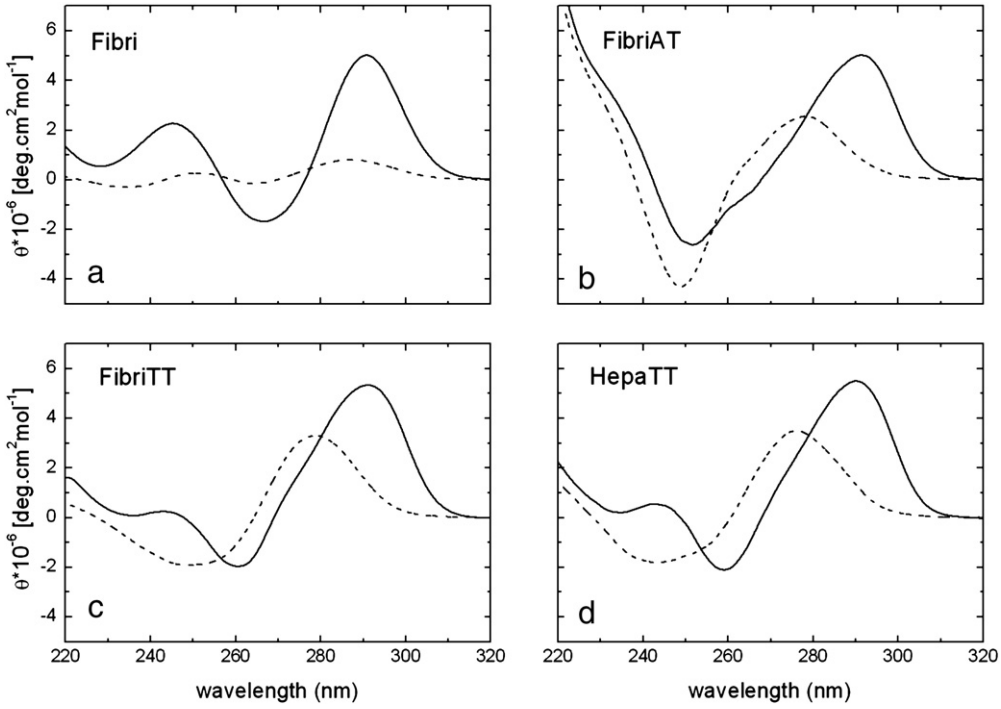

Fig. 2. CD spectra of original thrombin-binding aptamer Fibri (a) and individual components of thrombin-binding aptamer dimers (b, FibriAT; c, FibriTT; d, HepaTT) in the absence (dashed line) and presence of 50 mM KCl (solid line) in 10 mM Tris–HCl buffer, pH 7.4 at 25 °C. The concentration of oligonucleotides was 5 μM.

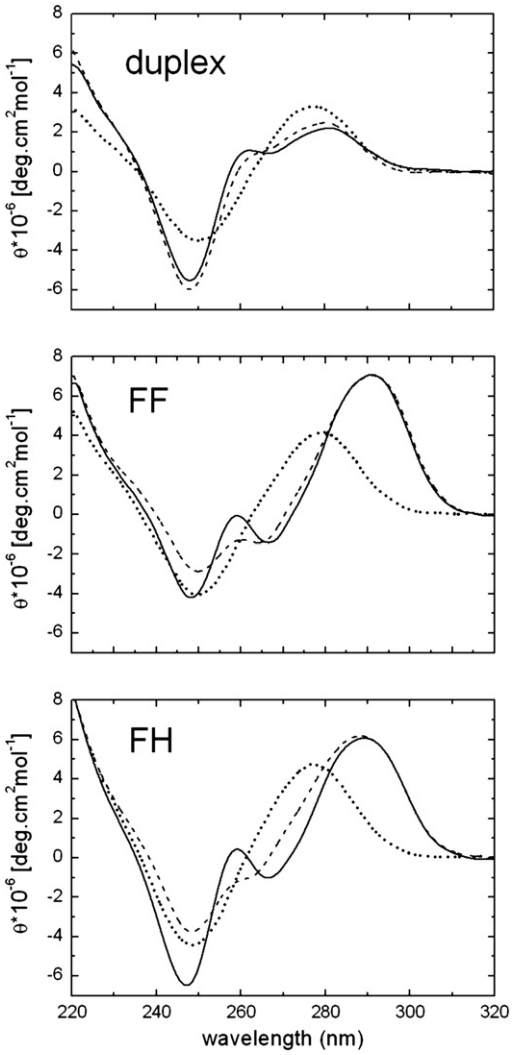

Fig. 3. CD spectra of flanked duplex sequence (duplex formed by hybridization of ODN-A and ODN-T) (a) and aptamer dimers (b, FF aptamer dimer; c, FH aptamer dimer) in 10 mM Tris–HCl buffer, pH 7.4 (dotted line), 10 mM Tris–HCl + 50 mM KCl, pH 7.4 (dashed line) and in binding buffer + 50 mM KCl, pH 7.4 (solid line) at 25 °C. Oligonucleotide concentration was 5 μM.

duplex conformation [22]. Hence, it can be suggested that the twiddle pattern observed on CD spectra for homodimer FF and heterodimer FH aptamers in binding buffer solution (Fig. 3b and c) reflects the hybridization of flanked sequences. Similarly to aptamer monomers, aptamer dimers are able to form quadruplex structure on their Fibri or Hepa heads. This can be recognized as sharp maximum at 292 nm for both dimers. Deep minimum around 265 nm usually observed for antiparallel guanine quadruplexes is overlapped by twiddle pattern indicating duplex formation. Again, lower ionic strength of 50 mM KCl was insufficient for complete hybridization (dashed line in Fig. 3b and c) and aptamer dimers are completely formed in 10 mM Tris +140 mM NaCl + 50 mM KCl, pH 7.4. In summary our results suggest that in appropriate conditions both types of aptamer dimers forms two G-quadruplex motifs on their Fibri and Hepa heads and are hybridized in duplex on their adenine and thymine tail ends. We suppose that such dimers would be able to bind thrombin and inhibit clot formation.

3.2. Differential scanning calorimetry studies

To study the thermal stability of dimers we performed DSC experiments. In the first series of DSC measurements we investigated the unfolding original 15-mer thrombin-binding aptamer (Fibri) and particular components of aptamer dimers – FibriTT, HepaTT, FibriAT. The transitions for these components are presented in Fig. 4a and corresponding thermodynamic parameters are shown in Table 2. In our experimental conditions the transitions are reversible as demonstrated by recovery of the original thermogram by rescanning the sample. Change of heating rate from 0.5 to 2 °C/min did not alter the thermodynamic parameters significantly, so the studied processes are not kinetically controlled. Fig. 4a shows the thermogram of Fibri 15-mer aptamers (solid line). As it can be seen, reversible monophasic transition has symmetric shape with temperature transition, T_m, of 44.8 °C. The integration of denaturation peak gives enthalpy changes $\Delta H = 35.3$ kcal/mol and determined changes of Gibbs energy, ΔG, is 2.2 kcal/mol. These values agree with those published earlier: 49.1 °C and 2.3 kcal/mol [15] or 53.0 °C and 1.9 kcal/mol [23], for T_m and ΔG, respectively. T_m value is smaller; certain deviations might be caused by different buffer solution used, in that the relatively high concentration of NaCl in our experiments and lower concentration of potassium. As we reported earlier [14] the presence of sodium ions has unfavorable influence on melting temperature and also on aptamer stability. The rest of DSC curves on Fig. 4a depict thermal unfolding of individual component forming aptamer dimers. The DSC curves have symmetric shape of monophasic transitions. The smaller peak belongs to FibriTT oligonucleotide (dashed line). Thermodynamic data presented in Table 2 obtained for FibriTT shows lower values of $\Delta G = 1.84$ kcal/mol and $T_m = 43.8$ °C in comparison with Fibri 15-mer. This indicates destabilizing effect of thymine tail end on quadruplex head [24]. On the contrary, FibriAT (dashed-dot line) has the most spacious peak area. Whereas FibriTT and FibriAT possess the same quadruplex head, the massive DSC peak of FibriAT suggests on influence of thymine-adenine tail end on the Fibri head. This modification affects the enthalpy change that is markedly higher than those for FibriTT. Considering high structural variability of quadruplexes we have applied Zuker's *mfold* algorithm for the prediction of alternative structures formation [25]. The evaluation shows that dimerization of very stable complex is likely. Five thymines and five adenines can form a stable DNA duplex connecting two FibriAT molecules (Fig. 5) [26]. Slowly moving and smear electrophoretic band of FibriAT confirms our suggestion, Fig. 5. Therefore, ΔH and ΔG are significantly higher in comparison with those of Fibri and FibriTT. This effect can be explained by the fact that unfolding consists of two separate unfolding processes having similar melting temperatures: G-quadruplex and duplex unfolding.

Thermograms for FibriTT and HepaTT have similar shape with nearly identical melting temperature, but of different stability. As it can be seen from Table 2, HepaTT has markedly favorable Gibbs energy change of 2.17 kcal/mol in comparison with those of FibriTT (1.84 kcal/mol). Considering that tail ends of both of oligonucleotides are the same and consist only of thymine bases it can be suggested that ΔG is affected by different G-quadruplex head. The reasons for this behavior might be connected with more complicated thermodynamics of Hepa head, which in contrast to the simple thermodynamic of Fibri, show concentration dependent thermodynamic characteristics [14].

Fig. 4b shows DSC curves of duplex part of aptamer dimers and single stranded ODN-A and ODN-T. ODN-T is composed of 20 thymines and does not exhibit any temperature dependent transition suggesting absence of DNA aggregates. On the other hand, ODN-A (dashed line) which possesses sequence of 15 adenines and 5 thymines displayed monophasic transition with $T_m = 38.8$ °C and low Gibbs energy change of 2.9 kcal/mol. It again indicates the presence of A–T pairing which can form either single molecule hairpin or homoduplexes in ODN-A (Fig. 5). Solid line at Fig. 4 represents thermogram of duplex part of aptamer dimers formed from ODN-A:ODN-T in molar ratio 1:1. Melting temperature and ΔG of duplex are considerably higher than those for ODN-A. This result also indicates that duplex solution contains only negligible population of compounds formed between two ODN-A strands.

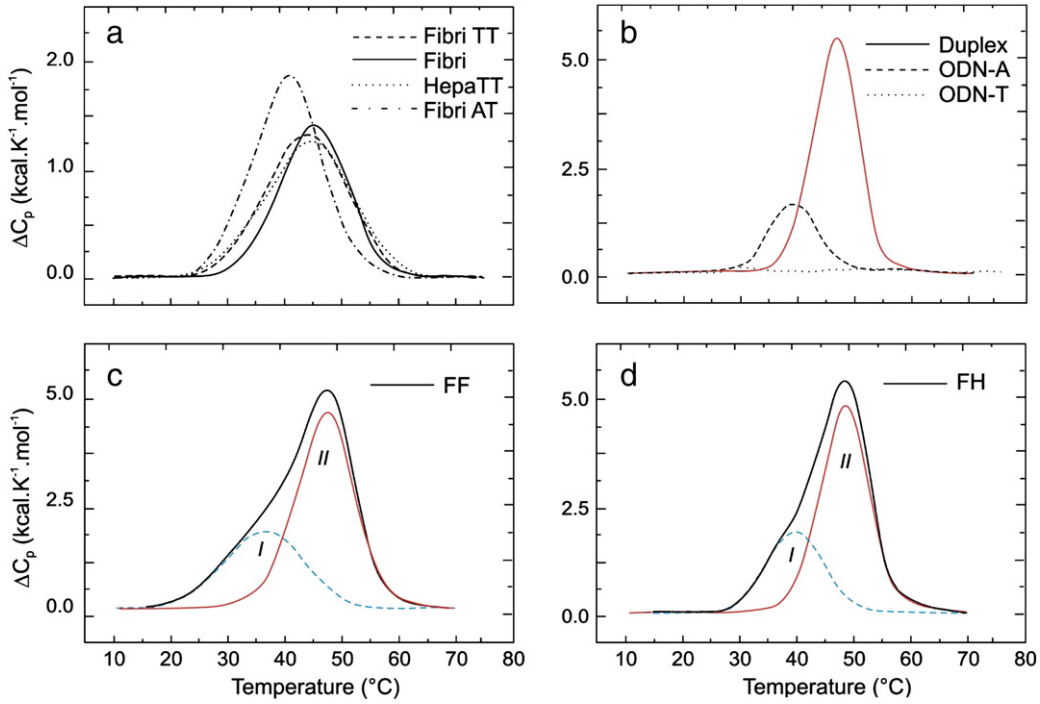

Fig. 4. DSC thermograms of (a) individual components of aptamer dimers (FibriTT, HepaTT and FibriAT) and canonical thrombin-binding aptamer Fibri (see Experimental section for aptamer compositions), (b) duplex part of aptamer dimer and single stranded ODN-T and ODN-A, (c) FF aptamer homodimer and (d) FH aptamer heterodimer in 10 mM Tris–HCl + 140 mM NaCl + 50 mM KCl buffer solution, pH 7.4. Oligonucleotide concentration was 250 μM and heating rate was 1 °C/min.

Interaction of FibriAT with FibriTT reveals aptamer dimer formation in FF. Thermogram of FF aptamer dimers, depicted on Fig. 4c, is characterized by more complex transition, which may be presented by superposition of two monophasic transitions. First transition is related to denaturation of two quadruplexes in heads of aptamer dimers and second transition belongs to duplex melting. The thermodynamic parameters for each transition are presented in Table 2. Obtained melting temperatures are similar to those of individual parts. Formation of aptamer dimers seems to have unfavorable effect on the heads stability. The Gibbs energy changes, ΔG, of the thermal transition corresponding to peak I belongs to two quadruplexes melting, so the ΔG value of one head in aptamer dimer is about 1.51 kcal/mol. This is markedly lower than for FibriAT or FibriTT alone. It can be predicted that ΔG of quadruplexes in aptamer dimer is affected by destabilizing effect of flanked duplex [24]. The stability of supporting duplex is however slightly better in the aptamer dimer configuration compared to the duplex alone, as is seen at transition peak II. This peak corresponds to the DNA duplex melting. It is seen in Table 2 that the transition II displays similar value of ΔG in comparison with duplex alone.

As with the homodimer, FH aptamer dimer denaturation yields an asymmetrical multiphasic DSC thermogram. Gaussian multi-peak fitting gives two individual two-state transitions. Comparison with acquired data for individual parts of aptamer dimer allows us to ascribe melting transition I consisted of both FibriAT and HepaTT quadruplex heads, and transition II corresponding to duplex denaturation. Similarly as described above the aptamer dimer formation exhibits decrease of T_m for FibriAT and HepaTT quadruplexes, markedly lower stability of Fibri and Hepa heads of aptamer dimers are observed in comparison with individual components (Table 2). This effect can be explained similarly to that presented above for FF aptamer dimers. Stability of duplex part of aptamer dimers is only slightly affected by presence of quadruplexes. Thus, the thermodynamic characteristics for both aptamer dimers are affected by presence of second quadruplex and the supporting

Table 2
Thermodynamic parameters for the denaturation processes in oligonucleotides and aptamer dimers in 10 mM Tris–HCl + 140 mM NaCl + 50 mM KCl buffer solution, pH 7.4 determined by differential scanning calorimetry. T_m, melting temperature; ΔH_{cal}, changes in enthalpy; ΔS_{cal}, changes in entropy; $\Delta G_{25\ °C} = \Delta H_{cal}\ (1 - T/T_m)$ are changes in Gibbs energy at $T = 25$ °C. Results represent mean ± S.D. obtained from 3 independent experiments in each series.

	T_m (°C)	ΔH_{cal} (kcal/mol)	ΔS_{cal} (cal/mol.K)	$\Delta G_{25\ °C}$ (kcal/mol)
Fibri	44.8 ± 0.2	35.3 ± 0.1	111 ± 5	2.20 ± 0.05
FibriAT	40.5 ± 0.1	53.3 ± 0.3	170 ± 5	2.64 ± 0.03
FibriTT	43.8 ± 0.2	31.1 ± 0.2	98 ± 3	1.84 ± 0.05
HepaTT	44.3 ± 0.1	34.8 ± 0.1	109 ± 2	2.17 ± 0.06
ODN-T	–	–	–	–
ODN-A	38.8 ± 0.1	65.8 ± 5.5	211 ± 5	2.91 ± 0.05
Duplex	46.3 ± 0.6	120.2 ± 5.5	376 ± 4	8.00 ± 0.05
FF aptamer dimer				
I.	38.1 ± 0.1	35.8 ± 0.5	115 ± 4	1.51 ± 0.04
II.	47.7 ± 0.1	121.1 ± 0.5	377 ± 4	8.56 ± 0.05
FH aptamer dimer				
I.	40.1 ± 0.3	36.0 ± 0.3	115 ± 5	1.74 ± 0.05
II.	48.5 ± 0.4	111.0 ± 0.1	345 ± 3	8.11 ± 0.06

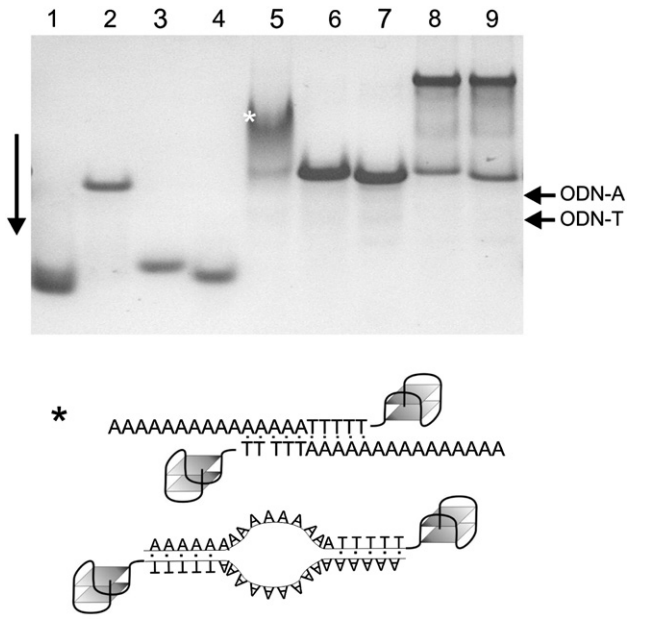

Fig. 5. Electrophoresis at 15 °C in 15% polyacrylamide gel in modified 25 mM Britton–Robinson buffer (pH 7.0) containing 50 mM KCl. Each well contains ~0.5 μM of DNA oligomer. In lines 1–9 there were loaded the following oligomers: (1) human telomeric repeats $(G_3T_2A)G_3$, (2) $(G_3T_2)G_3$, (3) Hepa, (4) Fibri, (5) FibriAT, (6) FibriTT, (7) HepaTT, (8) FibriAT:FibriTT (molar ratio 1:1), (9) FibriAT:HepaTT (1:1). Side arrows indicate the position of ODN-A and ODN-T. ODN-A:ODN-T duplex mobility is identical to ODN-A mobility. Asterisk in line 5 highlights the band which may represent the likely structures depicted under electrophoretic record calculated on base of Zuker's algorithm [26].

oligonucleotide part. However, both aptamer dimers exhibit sufficient thermal stability and thus can be used as potential thrombin inhibitors.

3.3. Electrophoretic measurements

Electrophoretic separation in non-denatured condition was applied for the confirmation of DNA aptamer molecularity. Standard PAGE clearly shows that Fibri, FibriTT, Hepa and HepaTT move in gel as one clear band, but the most intensive band of FibriAT moves more slowly than FibriTT. In addition, this band is smear (Fig. 5). This fact only supports our suggestion described above; there are more different conformational species present at given condition. Nevertheless, FF and FH complexes show similar mobilities corresponding to homo- and heterodimer molecule, respectively, but at ionic condition used in PAGE we still detect also the bands of unassociated FibriTT and/or FibriAT molecule (line 8) and HepaTT and/or HepaAT (line 9). Except standards, ODN-A, ODN-T and duplex ODN-A:ODN-T, also the human telomeric repeats $(G_3T_2A)G_3$ and the oligomer $(G_3T_2)G_3$ were used, lines 1 and 2 in Fig. 5. Human telomeric sequence forms monomolecular G-quadruplex and $(G_3T_2)G_3$ forms tetramolecular G-quadruplex structure in presence of potassium [19].

Increase of temperature causes dissociation of ODN-A:ODN-T duplex to ODN-A and ODN-T. This process is clearly observable by TGGE (Fig. 6). The same process is possible to observe for complexes FF and FH. DNA dissociation causes an increase of mobility because canonical structures move significantly faster than dimeric aptamers. TGGE does not allow using ionic strength 140 mM NaCl and 50 mM KCl due to a very high electric current during electrophoresis; therefore, only 50 mM KCl was used. Although melting temperature of DNA complex is about ~10 °C lower at this condition as it was at DSC measurements, this experiment clearly illustrates how dimeric complexes dissociate. However, the mobility difference between folded and unfolded quadruplex head of aptamer is significantly smaller; TGGE is not a sufficient method for the evaluation of aptamers used in this work. TGGE was applied for the first time for direct visualization of aptamer dimer dissociation.

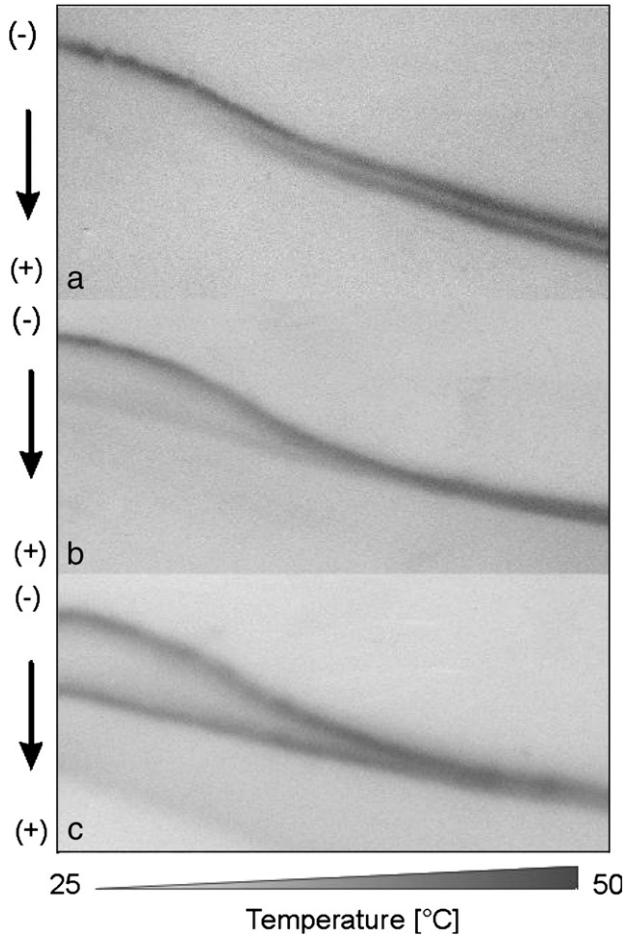

Fig. 6. TGGE of complexes (a) ODN-A:ODN-T, (b) FibriAT:FibriTT (1:1) and (c) FibriAT:HepaTT (1:2). In all the three records DNA complexes move more slowly than the dissociated canonical structures. The melting transition is accompanied by increasing mobility from native to denatured structure. The same electrophoretic buffer as at PAGE in Fig. 5 has been used. Separations were performed in 12% polyacrylamide gel.

3.4. Inhibitory activity measurements

To check whether formation of the quadruplex structure by aptamers and their thermal stability correlate with binding ability and inhibition of thrombin activity, we studied the thrombin-mediated fibrin gels formation in presence of aptamers. We investigated the inhibitory activity of two aptamer dimers – FF and FH – by comparing them with the canonical thrombin-binding aptamer Fibri in the absence and presence of potassium ions. The influence of potassium on inhibition ability is illustrated in Fig. 7. The column graph shows that absence of potassium caused only very small inhibition of thrombin-mediated fibrin gels formation for each of oligonucleotides. After addition of 50 mM KCl the ratio of coagulated fibrinogen strongly decreased. However, Fibri aptamer exhibits on average two-fold lower inhibition activity in comparison with aptamer dimers. The differences between inhibitory effect of Fibri aptamers and aptamer dimers were statistically significant according to the *t*-test with $p<0.01$. This is a rather interesting result considering the fact that guanine quadruplex, which is responsible for thrombin binding, has higher thermal stability in Fibri aptamers compared to those in aptamer dimers. However, obtained results on better inhibitory effect of aptamer dimers are in agreement with recent observation of improved binding properties of aptamer dimers to thrombin molecule in comparison with canonical aptamers [5]. The improved inhibitory effect of aptamer dimers is also in perfect agreement with results reported by Di Giusto and King [8] on the 2- to 3-fold improvement in anticoagulant effect of multivalent circular aptamers.

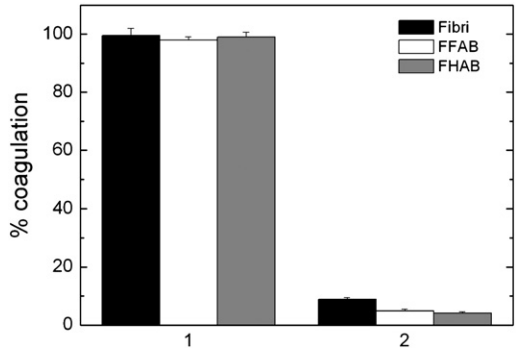

Fig. 7. The inhibitory activity of the monomer fibrinogen-binding site specific thrombin aptamers (Fibri) and two types of aptamer dimers – fibrinogen sensitive homodimers (FF) and fibrinogen-heparin sensitive heterodimers (FH) in the absence (1) and at presence of 50 mM potassium ions (2) in binding buffer, pH 7.4 at 25 °C. Measured clotting time was 75 min. Results represent mean ± S.D. obtained from 4 independent experiments in each series.

The inhibition of thrombin by aptamers strongly depends on the presence of potassium ions. This is due to essential role of potassium ions in quadruplex formation, which is the main binding motif of aptamers for both thrombin exosites. Previous studies showed that ligand binding to one exosite could induce allosteric changes at the opposite exosite [27]. It is possible that the interaction of Hepa quadruplex head with heparin-binding exosite might provoke allosteric changes at the fibrinogen-recognition exosite and conversely, interaction of Fibri head might reduce or improve the affinity of Hepa head. These effects can strongly modulate inhibition properties of FH aptamer dimer in comparison with FF aptamer dimer. However, comparable activity of FF homodimers and FH heterodimers suggests similar favorable effect of different quadruplex heads on thrombin molecule inhibition. Hence, the binding of Hepa quadruplex in FH aptamer dimer to heparin-binding exosites of thrombin effectively contributes to overall ability of inhibition of thrombin-mediated fibrin clot formation. In summary, our results displayed aptamer dimers as potent thrombin activity inhibitors.

4. Conclusion

We showed that the simple molecular engineering of DNA aptamers sensitive to the thrombin based on hybridization of their supporting part resulted in formation of aptamers dimers that maintain the 3D conformation of the binding site – the guanine quadruplexes. This has been shown in CD and DSC experiments. The aptamer dimers had higher affinity to the thrombin as it has been demonstrated by their approximately two-fold stronger inhibitory effect on cleavage the fibrinogen by thrombin in comparison with those of canonical monomeric aptamers. Thus, the molecular engineering can be used as effective tool for improvement the aptamer properties.

Acknowledgements

This work was supported by the Slovak Grant Agency (Projects No. 2/0038/09 to M.A., 1/0153/09 to V.V., and 1/0794/10 to T.H.), by Comenius University (Project No. UK/393/2009) and by SF EU 26220120021.

References

[1] A.D. Ellington, J.W. Szostak, In vitro selection of RNA molecules that bind specific ligands, Nature 346 (1990) 818–822.
[2] C. Tuerk, L. Gold, Systematic evolution of ligands by exponential enrichment: RNA ligands to bacteriophage T4 DNA polymerase, Science 249 (1990) 505–510.
[3] T. Hianik, J. Wang, Electrochemical aptasensors—recent achievements and perspectives, Electroanalysis 21 (2009) 1223–1235.
[4] M. Rimmele, Nucleic acid aptamers as tools and drugs: recent developments, Chembiochem 4 (2003) 963–971.
[5] T. Hianik, A. Porfireva, I. Grman, G. Evtugyn, Aptabodies—new type of artificial receptors for detection proteins, Protein Pept. Lett. 15 (2008) 799–805.
[6] H. Hasegava, K. Tiara, K. Sode, K. Ikebukuro, Improvement of aptamer affinity by dimerization, Sensors 8 (2008) 1090–1098.
[7] D. Michalowski, R. Chitima-Matsiga, D.M. Held, D.H. Burke, Novel bimodular DNA aptamers with guanosine quadruplexes inhibit hylogenetically diverse HIV-1 reverse transcriptases, Nucleic Acids Res. 36 (2008) 7124–7135.
[8] D.A. Di Giusto, G.C. King, Construction, stability and activity of multivalent circular anticoagulant aptamers, J. Biol. Chem. 279 (2004) 46483–46489.
[9] C.A. Holland, A.T. Henry, H.C. Whinna, F.C. Church, Effect of oligodeoxynucleotide thrombin aptamer on thrombin inhibition by heparin cofactor II and antithrombin, FEBS Lett. 484 (2000) 87–91.
[10] L.C. Bock, L.C. Griffin, J.A. Latham, E.H. Vermaas, J.J. Toole, Selection of single-stranded DNA molecules that bind and inhibit human thrombin, Nature 355 (1992) 564–566.
[11] P. Schultze, R.F. Macaya, J. Feigon, Three-dimensional solution structure of the thrombin-binding DNA aptamer d(GGTTGGTGTGGTTGG), J. Mol. Biol. 235 (1994) 1532–1547.
[12] K. Padmanabhan, K.P. Padmanabhan, J.D. Ferrara, J.E. Sadler, A. Tulinsky, The structure of α-thrombin inhibited by a 15-mer single-stranded DNA aptamer, J. Biol. Chem. 268 (1993) 17651–17654.
[13] D.M. Tasset, F.M. Kubik, W. Steiner, Oligonucleotide inhibitors of human thrombin that bind distinct epitopes, J. Mol. Biol. 272 (1997) 688–698.
[14] S. Ponikova, M. Antalik, T. Hianik, A circular dichroism study of the stability of guanine quadruplexes of thrombin DNA aptamers at presence of K^+ and Na^+ ions, Gen. Physiol. Biophys. 27 (2008) 271–277.
[15] B.I. Kankia, L.A. Marky, Folding of the thrombin aptamer into a G-quadruplex with Sr^{2+}: stability, heat and hydration, J. Am. Chem. Soc. 123 (2001) 10799–10804.
[16] S. Nagatoishi, Y. Tanaka, K. Tsumoto, Circular dichroism spectra demonstrate formation of the thrombin-binding DNA aptamer G-quadruplex under stabilizing-cation-deficient conditions, Biochem. Biophys. Res. Commun. 352 (2007) 812–817.
[17] Q. Wu, M. Tsiang, J.E. Sadler, Localization of the single-stranded DNA binding site in the thrombin anion-binding exosites, J. Biol. Chem. 34 (1992) 24408–24418.
[18] C. Antonacci, J.B. Chaires, R.D. Sheardy, Biophysical characterisation of the human telomeric $(TTAGGG)_4$ repeat in a potassium solution, Biochemistry 46 (2007) 4654–4660.
[19] V. Viglasky, L. Bauer, K. Tluckova, Structural features of intra- and intermolecular G-quadruplexes derived from telomeric repeats, Biochemistry 49 (2010) 2110–2120.
[20] M. Lu, Q. Guo, N.R. Kallenbach, Thermodynamics of G-tetraplex formation by telomeric DNAs, Biochemistry 32 (1993) 598–601.
[21] I. Smirnov, R.H. Shafer, Effect of loop sequence and size on DNA aptamer stability, Biochemistry 39 (2000) 1462–1468.
[22] G. Luck, H. Triebel, M. Waring, C. Zimmer, Conformational dependent binding of netropsin and distamycin to DNA and DNA model polymers, Nucleic Acids Res. 1 (1974) 503–530.
[23] B. Pagano, L. Martino, A. Randazzo, C. Giancola, Stability and binding properties of a modified thrombin binding aptamer, Biophys. J. 94 (2008) 562–569.
[24] V. Viglasky, L. Bauer, K. Tluckova, K.P. Javorsky, Evaluation of human telomeric G-quadruplexes: the influence of overhanging sequences on quadruplex stability and folding, J. Nucleic Acids (2010), pii: 820356.
[25] C.C. Hardin, A.G. Perry, K. White, Thermodynamic and kinetic characterization of the dissociation and assembly of quadruplex nucleic acids, Biopolymers 56 (2000–2001) 147–194.
[26] N.R. Markham, M. Zuker, DINAMelt web server for nucleic acid melting prediction, Nucleic Acids Res. 33 (2005) W577–W581.
[27] J.H. Fredenburgh, A.R. Stafford, J.I. Weitz, Evidence for allosteric linkage between exosites 1 and 2 of thrombin, J. Biol. Chem. 272 (1997) 25493–25499.